Crystal and Molecular Structure of Dodecamethoxycyclohexaphosphazene: Non-bonded Interactions and Conformation

By **Maryon W. Dougill,*** Department of Pure and Applied Chemistry, The Polytechnic, Huddersfield, Yorks
Norman L. Paddock, Department of Chemistry, University of British Columbia, Vancouver 8, British Columbia, Canada

Crystals of the title compound are monoclinic, $a = 11{\cdot}434$, $b = 12{\cdot}891$, $c = 9{\cdot}805$ Å (all ±0·008 Å), $\beta = 104{\cdot}5 \pm 0{\cdot}1°$, $Z = 2$, space group $P2_1/n$. The structure was determined from photographic data by Patterson and Fourier methods and refined three dimensionally to R 0·11 for 2228 observed reflections. The molecule is centrosymmetric and has a double-tub conformation, in which all the ring bonds are equal in length (1·567 Å); ring N–P–N angles are 114·4—121·6° (mean 118·5°), and P–N–P angles 133·4—135·1° (mean 134·3°). The detailed stereochemistry is similar to that of phosphate diesters. The angles at phosphorus, the conformation of the ring, and the orientation of the methoxy-groups are inter-related, and are discussed in terms of non-bonded interactions, including polar contributions.

ALTHOUGH the crystal structures of many homogeneously substituted phosphazenes based on six- and eight-membered rings have been determined, there is less information about the larger cyclic compounds. The three molecules $N_5P_5Cl_{10}$,[1] $N_5P_5Br_{10}$,[2] and $N_6P_6(NMe_2)_{12}$ [3] all have distinctive structural features, but the factors controlling ring geometry are still incompletely understood. We now report details of the structure of dodecamethoxycyclohexaphosphazene $N_6P_6(OMe)_{12}$. A comparison with the structures of the related molecules $N_4P_4(OMe)_8$ (ref. 4) and $N_8P_8(OMe)_{16}$ (ref. 5) brings out features of general importance.

EXPERIMENTAL

Crystal Data.—$C_{12}H_{36}N_6O_{12}P_6$, $M = 642{\cdot}3$, Monoclinic, $a = 11{\cdot}434$, $b = 12{\cdot}891$, $c = 9{\cdot}805$ Å, all $\pm 0{\cdot}008$ Å, $\beta = 104{\cdot}5 \pm 0{\cdot}1°$, $U = 1389{\cdot}6$ Å^3, $D_m = 1{\cdot}54$, $Z = 2$, $D_c = 1{\cdot}532$ g cm^{-3}, $F(000) = 672$. Space group $P2_1/n$ (No. 14), molecular symmetry $\bar{1}$, Cu-K_α radiation, μ(Cu-K_α) $= 41$ cm^{-1}.

Equant crystals of the title compound [6] were obtained from its solution in carbon tetrachloride. Cell dimensions were obtained from oscillation and Weissenberg photographs. Intensities were estimated visually from multiple-film, equi-inclination Weissenberg photographs for layers 0—7*kl*, *h*0—5*l*, and *hk*0—2; of a possible 2600 reflections, 2228 had measurable intensities. Lorentz and polarisation corrections were calculated and applied by use of a KDF 9 computer at Leeds University; the intercorrelation of the layers was carried out on a desk machine. Atomic scattering factors were taken from ref. 7. The weighting scheme used for the structure-factor least-squares programme was $\omega^{\frac{1}{2}} = 1/(p_1 + |F_o| + p_2|F_o|^2 + p_3|F_o|^3)^{\frac{1}{2}}$, with $p_1 = 10$, $p_2 = 0$, and $p_3 = 0{\cdot}01$ throughout.

Structure Determination.—The positions of the three independent phosphorus atoms were derived from the P · · · P vector peaks in the three-dimensional sharpened Patterson synthesis; R for the structure factors based on the co-ordinates of these atoms was 0·48. The positions of the other atoms were found on a three-dimensional electron-density synthesis. Their co-ordinates were refined by alternate structure-factor and electron-density syntheses until R was reduced to 0·24. Five cycles of block-diagonal least-squares refinement, with individual isotropic temperature factors, reduced R to 0·123. A further three cycles refined the atomic co-ordinates and the anisotropic temperature factors, to give a final R of 0·108 (for observed reflections only). At this stage the parameter shifts were *ca.* 0·1σ, and refinement was considered to be complete. The hydrogen atoms were not located. Measured and calculated structure factors are listed in Supplementary Publication No. SUP 20944, (12 pp., 1 microfiche).†

RESULTS

Final atomic co-ordinates and thermal parameters, with their standard deviations, are given in Tables 1 and 2, and the molecular dimensions in Table 3. The torsion

---

† See Notice to Authors No. 7 in *J.C.S. Dalton*, 1973, Index issue.

[1] A. W. Schlueter and R. A. Jacobson, *J. Chem. Soc. (A)*, 1968, 2317.

[2] J. G. Hartsuiker and A. J. Wagner, *J.C.S. Dalton*, 1972, 1069.

[3] A. J. Wagner and A. Vos, *Acta Cryst.*, 1968, **B24**, 1423.

[4] G. B. Ansell and G. J. Bullen, *J. Chem. Soc. (A)*, 1971, 2498.

[5] N. L. Paddock, J. Trotter, and S. H. Whitlow, *J. Chem. Soc. (A)*, 1968, 2227.

[6] F. Rallo, *Ricerca sci.*, 1965, **7**, 1134.

[7] 'International Tables for *X*-Ray Crystallography,' vol. 3, Kynoch Press, Birmingham, 1962.

angles about the individual phosphorus atoms, which define the conformation, are given in Table **4**. **Figure 1** shows

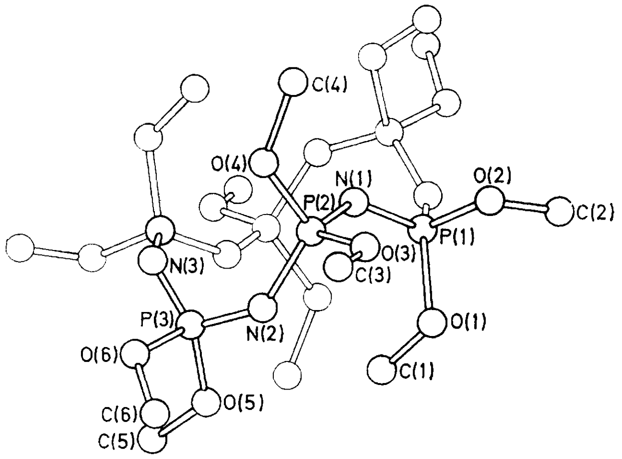

FIGURE 1 General view of $N_6P_6(OMe)_{12}$

that the conformation of the molecule is a double tub, the two parts being related by a centre of symmetry. The general arrangement of the molecules in the cell is shown in Figure 2, which (with Table 5) includes also the closest non-bonded distances.

TABLE 1

Atomic co-ordinates, fractions of the cell edge, with standard deviations (10^{-3} Å) in parentheses

	x/a	$\sigma(x)$	y/b	$\sigma(y)$	z/c	$\sigma(z)$
P(1)	0·2246	2	0·0380	2	0·1062	2
P(2)	0·0328	2	0·1413	2	0·1967	2
P(3)	−0·1663	2	0·0025	2	0·1928	2
O(1)	0·2467	6	−0·0460	6	0·2280	6
O(2)	0·3363	6	0·1120	7	0·1651	6
O(3)	0·1247	6	0·1938	6	0·3269	6
O(4)	−0·0533	6	0·2315	6	0·1212	7
O(5)	−0·1324	5	−0·1151	6	0·2353	6
O(6)	−0·2623	6	0·0317	7	0·2765	6
N(1)	0·1063	7	0·1024	8	0·0921	7
N(2)	−0·0459	7	0·0630	8	0·2566	7
N(3)	−0·2364	7	0·0151	7	0·0346	7
C(1)	0·1671	10	−0·1354	10	0·2125	10
C(2)	0·4582	10	0·0795	14	0·1753	13
C(3)	0·0807	11	0·2465	12	0·4345	11
C(4)	−0·0075	13	0·3137	11	0·0479	13
C(5)	−0·2253	12	−0·1921	10	0·1994	12
C(6)	−0·2268	12	0·0346	13	0·4292	10

TABLE 2

Thermal parameters,[a] with standard deviations in parentheses

	U_{11}	U_{22}	U_{33}	$2U_{23}$	$2U_{31}$	$2U_{12}$
P(1)	27(1)	34(1)	33(1)	−5(2)	20(2)	−1(2)
P(2)	27(1)	32(1)	35(1)	−4(2)	18(2)	−3(2)
P(3)	26(1)	31(1)	32(1)	0(2)	24(1)	0(2)
O(1)	44(3)	47(3)	41(3)	11(5)	22(5)	9(6)
O(2)	39(3)	51(4)	52(4)	−21(6)	31(6)	−13(6)
O(3)	42(3)	51(3)	42(3)	−18(6)	15(5)	−21(6)
O(4)	41(3)	40(3)	60(4)	4(6)	46(6)	17(5)
O(5)	32(3)	35(3)	44(3)	19(5)	9(5)	0(5)
O(6)	33(3)	55(4)	43(4)	−10(6)	28(5)	17(6)
N(1)	47(4)	53(4)	44(4)	−4(7)	37(6)	7(7)
N(2)	43(4)	55(4)	42(4)	−3(7)	30(6)	−15(7)
N(3)	41(4)	37(3)	43(4)	3(6)	29(6)	10(6)
C(1)	60(6)	47(5)	56(6)	4(9)	54(8)	−22(9)
C(2)	37(5)	96(9)	78(8)	−14(14)	25(10)	−24(11)
C(3)	74(7)	67(7)	51(6)	−41(10)	27(10)	−9(12)
C(4)	93(8)	44(5)	73(7)	37(10)	38(13)	−14(11)
C(5)	78(7)	41(5)	71(7)	6(9)	23(11)	−29(10)
C(6)	73(7)	89(8)	35(5)	−10(10)	39(9)	25(13)

[a] $f = f_0 \exp[-2\pi^2(U_{11}h^2a^{*2} + U_{22}k^2b^{*2} + U_{33}l^2c^{*2} + 2U_{23}klb^*c^* + 2U_{31}lhc^*a^* + 2U_{12}hka^*b^*)]$.

TABLE 3

Bond lengths (Å) and angles (°), with standard deviations in parentheses

(*a*) Distances			
P(1)–N(3′)	1·576(7)	P(2)–O(4)	1·582(6)
P(1)–N(1)	1·563(8)	P(3)–O(5)	1·594(6)
P(2)–N(1)	1·563(8)	P(3)–O(6)	1·572(6)
P(2)–N(2)	1·561(8)		
P(3)–N(2)	1·570(8)	O(1)–C(1)	1·452(12)
P(3)–N(3)	1·566(7)	O(2)–C(2)	1·434(12)
		O(3)–C(3)	1·448(13)
P(1)–O(1)	1·585(7)	O(4)–C(4)	1·449(13)
P(1)–O(2)	1·584(6)	O(5)–C(5)	1·432(12)
P(2)–O(3)	1·588(6)	O(6)–C(6)	1·450(11)
(*b*) Angles			
P(1)–O(1)–C(1)	119·1(6)	O(5)–P(3)–O(6)	104·3(3)
P(1)–O(2)–C(2)	122·0(7)		
P(2)–O(3)–C(3)	120·3(6)	N(3′)–P(1)–O(4)	109·3(4)
P(2)–O(4)–C(4)	120·7(6)	N(3′)–P(1)–O(2)	110·0(4)
P(3)–O(5)–C(5)	118·6(6)	N(1)–P(1)–O(1)	113·6(4)
P(3)–O(6)–C(6)	119·6(6)	N(1)–P(1)–O(2)	108·3(4)
P(1)–N(1)–P(2)	135·1(5)		
P(2)–N(2)–P(3)	134·5(5)	N(1)–P(2)–O(3)	107·9(4)
P(3)–N(3)–P(1′)	133·4(5)	N(1)–P(2)–O(4)	107·6(4)
		N(2)–P(2)–O(3)	107·5(4)
N(3′)–P(1)–N(1)	114·4(4)	N(2)–P(2)–O(4)	107·6(4)
N(1)–P(2)–N(2)	119·6(4)		
N(2)–P(3)–N(3)	121·6(4)	N(2)–P(3)–O(5)	103·7(4)
		N(2)–P(3)–O(6)	109·3(4)
O(1)–P(1)–O(2)	100·1(3)	N(3)–P(3)–O(5)	112·9(4)
O(3)–P(2)–O(4)	105·8(3)	N(3)–P(3)–O(6)	104·0(4)

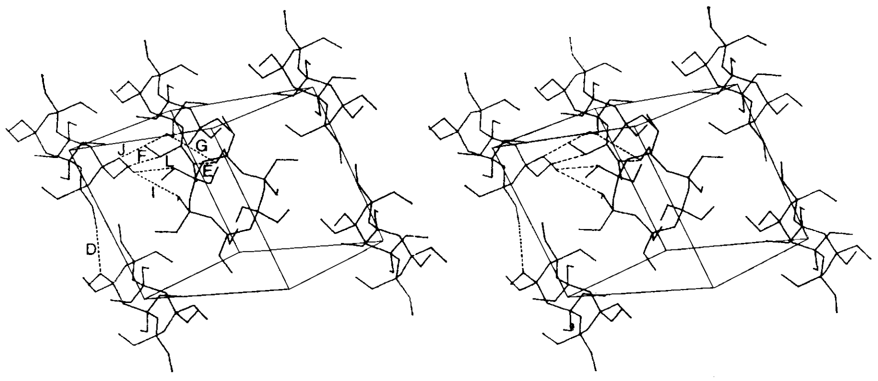

FIGURE 2 Stereoscopic view of the packing of the molecules in the cell

TABLE 4

Torsion angles (°) about individual phosphorus atoms

Axis	Angle *	Axis	Angle *
O(1)–P(1)	−175·9	N(1)–P(2)	−74·9
O(2)–P(1)	67·9	N(2)–P(2)	−70·6
N(3′)–P(1)	12·6		
N(1)–P(1)	158·7	O(5)–P(3)	62·3
		O(6)–P(3)	65·1
O(3)–P(2)	58·8	N(2)–P(3)	−0·8
O(4)–P(2)	68·7	N(3)–P(3)	85·1

* Angles measured anticlockwise; reference planes shown in Figure 6.

DISCUSSION

We comment on three aspects of the structure: the extent and nature of the π-bonding, the conformations of the ring and the exocyclic groups, and correlations between the bond angles at phosphorus. The mean molecular parameters of $N_6P_6(OMe)_{12}$ are summarised in Table 6, and compared with those of $N_4P_4(OMe)_8$ and $N_8P_8(OMe)_{16}$. Except for the O–P–O and N–P–N angles (see later) individual bond lengths and angles do not differ significantly from their mean values.

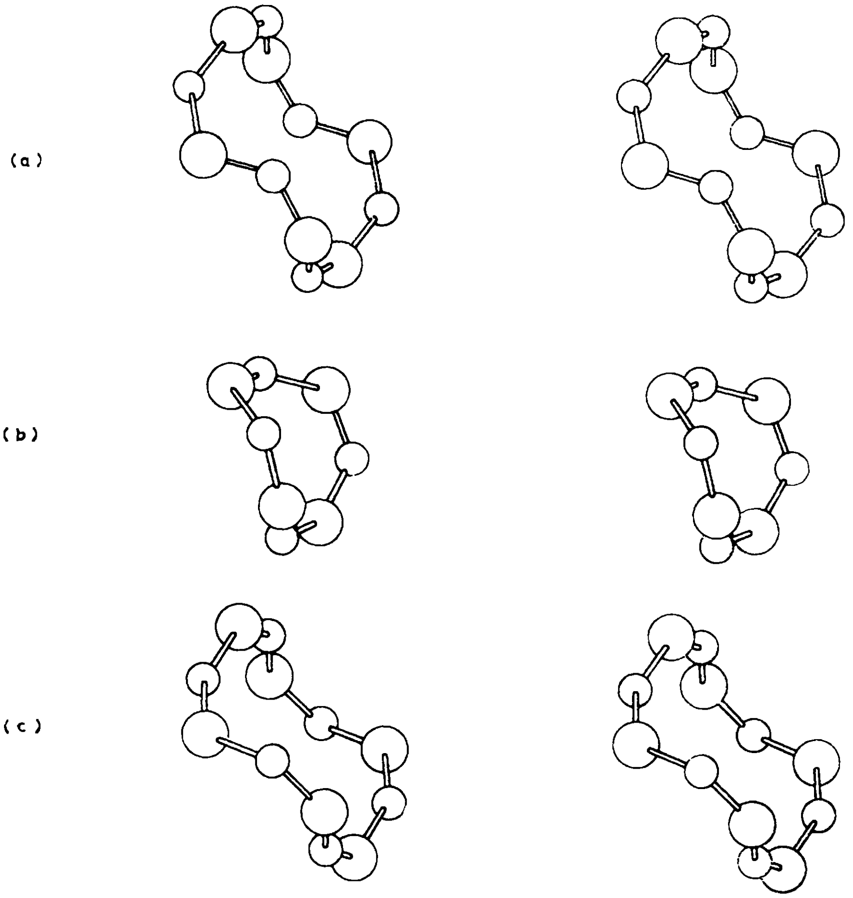

FIGURE 3 Stereoscopic views of the skeletal structures of (a) $N_6P_6(OMe)_{12}$, (b) $N_4P_4Cl_8$, and (c) $N_6P_6(NMe_2)_{12}$

TABLE 5

Short inter- and intra-molecular distances [a] (Å)

C(2) (001) [b]–O(6) (101)	3·16 (D)
O(3) (000)–C(1) (½−, ½+, ½−)	3·33 (G)
O(4′) (000)–C(6′) (001)	3·43 (F)
O(2) (000)–C(1) (½−, ½+, ½−)	3·47 (E)
C(5) (001)–O(4) (½+, ½−, ½+)	3·56 (I)
C(3) (000)–O(5′) (001)	3·57 (J)
C(3) (001)–O(6) (½+, ½−, ½+)	3·57 (L)
O(2)–O(3)	3·38
O(1)–O(3)	3·62
C(1)–O(5)	3·50
C(1)–C(4′)	3·58
C(1)–O(4′)	3·43

[a] Distances between exocyclic atoms less than 3·6 Å. Letters D—L refer to Figure 2. [b] Co-ordinates of molecular centre.

TABLE 6

Mean geometries of methoxyphosphazenes [a]

	$N_4P_4(OMe)_8$	$N_6P_6(OMe)_{12}$	$N_8P_8(OMe)_{16}$
P–N	1·570	1·567	1·561
P–O	1·581	1·584	1·576
O–C	1·42	1·444	1·440
N–P–N	121·0	118·5	116·7
P–N–P	132·2	134·3	136·7
O–P–O	105·5	103·4	101·3
P–O–C	121·0	120·1	120·6

[a] Bond lengths (Å), angles (°).

The P–N and P–O bond lengths and the mean P–O–C bond angles are consistent with the presence of substantial π-bonding in the ring, and with less in the exocyclic groups. The bond lengths do not indicate any large variation of π-bonding with ring size, though the correlated reduction in N–P–N and increase in P–N–P with increasing ring size suggest that the bonding electron density tends to concentrate near nitrogen as the restraints imposed by cyclisation are reduced. The effects of non-bonded interactions are discussed later. The two π-components are evidently approximately equal in the N_6P_6 ring, since no structural peculiarity depending on their inequality could be detected; the same conclusion was reached for $N_4P_4Me_8H^+$, which has two different conformations within the same unit cell.[8]

The conformation of $N_6P_6(OMe)_{12}$ appears to be controlled mainly by non-bonded interactions. Its skeletal structure (Figure 3a) is qualitatively similar to that of $N_6P_6(NMe_2)_{12}$[3] (Figure 3c), but the comparatively close approach (3·73 Å) of the symmetrically related nitrogen atoms N(1), N(1′), results in an elongation of the molecule in the direction P(3) ··· P(3′) [expressed in the distances N(1) ··· N(3) 3·98, N(1) ··· N(2′) 3·94, and N(3) ··· N(2′) 4·92 Å], the three-fold symmetry being lost. The molecule can be regarded as a double tub, the conformation of the seven-atom fragments N(1),P(2),N(2),P(3),N(3),P(1′),N(1′) and its symmetrically related counterpart being similar to that of $N_4P_4Cl_8$,[9] shown in Figure 3b in an equivalent orientation. The characteristic of the tub conformation is that neighbouring PX_2 groups are mutually staggered, and the qualitative conclusion that steric repulsions between them are then minimised is supported numerically.[10] Views along successive P ··· P vectors in $N_6P_6(OMe)_{12}$ are shown in Figure 4. The configurations are almost ideally staggered for P(2) ··· P(3) and P(3) ··· P(1′), but less so for P(1) ··· P(2), these phosphorus atoms being in different tubs.

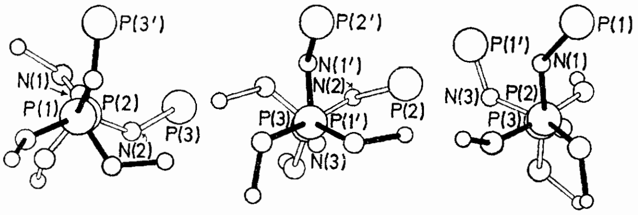

FIGURE 4 Views along P ··· P vectors in $N_6P_6(OMe)_{12}$, showing staggering of shaded relative to unshaded bonds from phosphorus

The need for a closer examination of non-bonded interactions is apparent from some other structure determinations.[3,4] While the simple qualitative concept of atom repulsion is useful, it cannot explain some of the systematic relationships. On the other hand, minimisation of the total conformational energy of such a large molecule seems out of the question at present, and we therefore take a middle course, relying on numerical calculations on fragments of the molecule for guidance as to its total behaviour. Earlier,[5] the stereochemistry of the $(PN)_2P(OMe)_2$ group was considered in terms of the repulsive interactions within an idealised $P(XY)_4$ molecule, PXY < 180° (Figure 5a).

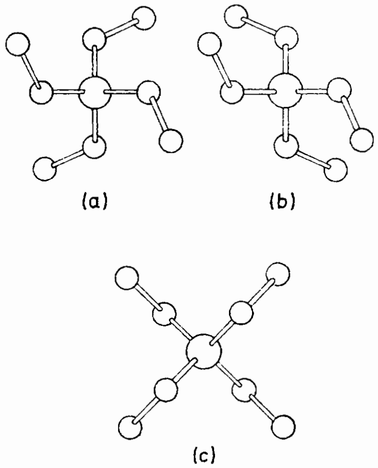

FIGURE 5 Idealised $P(XY)_4$ molecules (a) *M1*, torsion angles 60, 60, − 60, − 60°; (b) *M2*, torsion angles all 60°; and (c) *M2*, torsion angles all 180°; (b) and (c) are identical conformations in different orientations (see text and Figure 6)

The intuitive idea that its conformational energy is minimised when all the bonds are mutually staggered, the ideal molecule then having $\bar{4}$ symmetry (Figure 5a), is justified by calculation (see later). Each pair of XY groups is then related either by an inverse tetrad (gauche-*trans*, *GT*) or a diad axis (*GG*).* The qualitative distinction remains as the symmetry is lowered, and the majority of the immediate environments of the phosphorus atoms in $N_4P_4(OMe)_8$, $N_6P_6(OMe)_{12}$, and $N_8P_8(OMe)_{16}$ correspond to this approximate description. Even when they do not, the conformations of the diester groups by themselves are all either *GG* or *GT*, as are those of most phosphate diesters. We therefore consider the following models in greater detail: (1) the fragment $N_2P(OMe)_2$, to determine the relative importance of the different atomic interactions in the simplest realistic case; (2) an idealised $P(OMe)_4$ molecule, to investigate the interactions of four angular groups over the whole range of torsion angles; and (3) a less symmetrical model, $(MeO)_2P(NMe)_2$, used to explore the effect of variation of potential functions on the stability of the stable conformations of $P(OMe)_4$. The justification for the treatment of the molecule as a set of such idealised fragments is its success in accounting for the

---

* Terminology from Mizushima.[11] *GT* and *GG* conformation are the Type 1 and Type 2 referred to earlier,[5] or *sc*, *ap* and *sc*, *sc* in the nomenclature of Klyne and Prelog.[12] The *GG*, *GT*, and *TT* conformations are illustrated in Figure 7.

[8] J. Trotter, S. H. Whitlow, and N. L. Paddock, *Chem. Comm.*, 1969, 695; J. Trotter and S. H. Whitlow, *J. Chem. Soc.* (*A*), 1970, 460.

[9] R. Hazekamp, T. Migchelsen, and A. Vos, *Acta Cryst.*, 1962, **15**, 539.

[10] K. A. R. Mitchell and N. L. Paddock, unpublished calculations.

[11] S. Mizushima, ' Structure of Molecules and Internal Rotation,' Academic Press, New York, 1954.

[12] W. Klyne and V. Prelog, *Experientia*, 1960, **16**, 521.

main qualitative features of the three structures. A full treatment would need to include at least those intergroup interactions which give the short interatomic distances of Table 5, but the angular distortions which they cause apparently do not invalidate the general arguments given here.

The potential functions used are given in Table 7, and the angular conventions in Figure 6. In the fragment $N_2P(OMe)_2$, if only Me · · · Me interactions are included, small torsion angles lead to prohibitively large repulsive interactions, but there is otherwise no effective conformational preference. The addition of Me–O interactions stabilises the $\tau_1 = \tau_2$ conformations, but the main effect is to destabilise the *cis–trans* (0,180°; *CT*) conformation. The Me · · · N interactions become increasingly attractive as τ_1, τ_2 are reduced, another effect being a large repulsive interaction near τ_1, τ_2 120°. The potential map including the three interactions shows three well defined minima, which, for the A_1 constants (Table 7), are [τ_1, τ_2 (°), V (kcal mol^{-1})] *GG* (62, 62, −0·31), *GT* (53, 180, −0·72), and *TT* (180, 180, −0·80). The use of the A_2 constants increases the energy differences without altering the order. The three ideal conformations are illustrated in Figure 7, and the actual conformations in $N_6P_6(OMe)_{12}$ in Figure 8.

TABLE 7

Interatomic potential constants [a,b,c]

Interaction	B	A_1	A_2
Me · · · Me	3·4333	3·4979 (4·0)	3·6686 (4·4)
Me · · · O	2·8930	2·9603 (3·4)	3·1296 (3·8)
Me · · · N	3·2527	3·1847 (3·5)	3·3618 (3·9)
O · · · O	2·4605	2·4775 (2·8)	2·6485 (3·2)
O · · · N	2·7421	2·6617 (2·9)	2·8393 (3·3)
N · · · N	2·4605	2·8699 (3·0)	3·0552 (3·4)

[a] Potential $V = (A/r)^{12} - (B/r)^6$, kcal mol^{-1} for r in Å. Constants by method of R. A. Scott and H. A. Scheraga (*J. Chem. Phys.*, 1965, **42**, 2209); B from Slater–Kirkwood expression, A by minimisation of V at interatomic distance (Å) shown in parentheses. A_1 corresponds to normal van der Waals separations, A_2 to those with radii increased by 0·2 Å (D. A. Brant, W. G. Miller, and P. J. Flory, *J. Mol. Biol.*, 1967, **23**, 47), to allow for the difference between the equilibrium distances of a pair of atoms when isolated and when in a condensed phase (M. L. Huggins, in ' Structural Chemistry and Molecular Biology,' eds. A. Rich and N. Davidson, Freeman, San Francisco, 1968, p. 761). [b] Potential functions of the ' 6-exp ' as well as the ' 6-12 ' type were occasionally used, but the results were insignificantly different, and did not justify the additional flexibility of a three-constant formula. [c] Polar contributions were calculated separately, rather than included in all potential calculations [see Scott and Scheraga, footnote (*a*)]. The torsional barrier to rotation about a P–O bond is believed to be small, and its contribution to the potential was ignored.

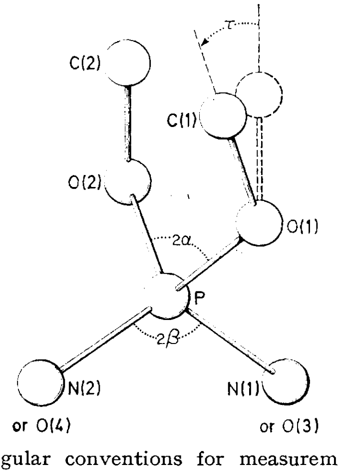

FIGURE 6 Angular conventions for measurement of torsion angles in $N_2P(OMe)_2$ and in $P(OMe)_4$. Torsion angles τ_1, τ_2 about O(1)–P, O(2)–P are measured from the position in which C(1),O(1),P,O(2),C(2) are coplanar. Torsion angles τ_3, τ_4 about N(1)–P, N(2)–P defined similarly relative to the plane N(1),P,N(2)

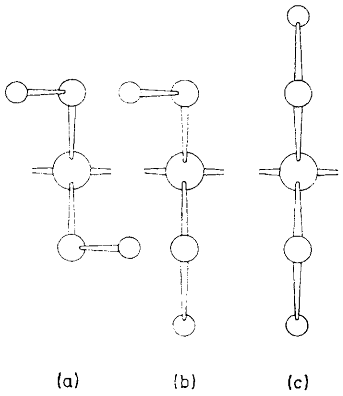

FIGURE 7 Idealised conformations (a) *GG*, (b) *GT*, and (c) *TT*

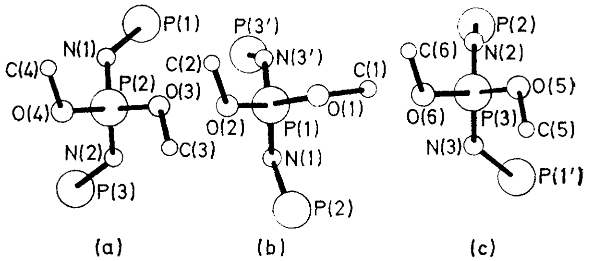

FIGURE 8 Local conformations in $N_6P_6(OMe)_{12}$ at (a) P(2), (b) P(1), and (c) P(3)

Although the *TT* conformation is apparently of lowest energy, it does not occur in the methoxyphosphazenes, and is rare in other phosphate diesters.[13-15] Sundaralingam[14] has pointed out that the lone-pair moment at oxygen (which would be reinforced by the polarities of the P–O and C–O bonds) would destabilise *TT*, and our calculations confirm this. By themselves, however, these interactions, simulated by point dipoles at oxygen, exaggerate the difference between *GG* and *GT*, and we have obtained better results by placing partial positive and negative charges on methyl and oxygen respectively. For one particular choice, which nearly equalises the *GG* and *GT* energies, the final

---

[13] E. Shefter, M. Barlow, R. A. Sparks, and K. N. Trueblood, *Acta Cryst.*, 1969, **B25**, 895.

[14] M. Sundaralingam, *Biopolymers*, 1969, **7**, 821.

[15] Y. Kyogoku and Y. Iitaka, *Acta Cryst.*, 1966, **21**, 49.

energy map is shown in Figure 9, which includes also the torsion angles of the three methoxyphosphazenes. The relative energies of the three well defined independent minima, and their populations, suggest that the conformations of the $P(OMe)_2$ groups are a consequence of normal non-bonded interactions, polar contributions being included. The energy differences are small (smaller still if A_1 constants are used), consistent with the spectroscopic evidence for rotational isomerism in related compounds.[16] Conformational preferences in substituted phosphazenes carrying bulkier ester groups are therefore likely to be less marked. The assumed polarities (of the order of 1D), although reasonable, are not unique, and, because of ignorance of the total charge distribution, the polar interactions are known less accurately than the van der Waals potentials. Whether introduced as point dipoles or as partial charges, however, they vary comparatively slowly with distance, and their general effect is to leave the approximate angular co-ordinates of maxima and minima unchanged, simply altering the energies of conformationally remote structures. Although the *GG* torsion angles are calculated correctly, the calculated *G* angle in the *GT* conformation is too small (Figure 9). This arises from various imperfections in the treatment, the most important being the use of an average N_2PO_2 geometry, which is not simultaneously appropriate for both the *GG* and *GT* conformations, and also the detailed dependence of the local conformation on four, rather than two, bent groups attached to phosphorus.

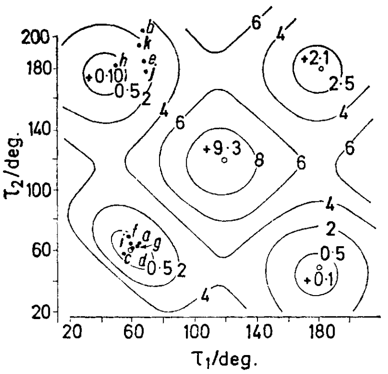

FIGURE 9 Potential-energy contours (kcal mol^{-1}) of $N_2P(OMe)_2$ as a function of τ_1, τ_2, relative to *GG* conformation near 60, 60°. Conformations of methoxy-groups in phosphazenes (solid circles) *a*—*d*, $N_4P_4(OMe)_8$, P(1)—(4); *e*—*g*, $N_6P_6(OMe)_{12}$, P(1)—(3); *h*—*k*, $N_8P_8(OMe)_{16}$, P(1)—(4)

The non-bonded interactions within the whole $(PN)_2P(OMe)_2$ fragment are less reliably treated, because interactions from other methoxy-groups are significant. Because of its likely applicability and similarity to molecules of known structure, we have investigated the model molecule $P(OMe)_4$, initially with tetrahedral angles at phosphorus. Even with this simplification, minimisation of energy with respect to the four torsion angles is computationally excessive. However, the lowest-four minima remain unchanged as the angular step is reduced to 30°, the smallest interval used for variation of the τ values over the range 0—360°. The conformation of lowest energy (for either A_1 or A_2 constants) is that of Figure 5a (τ_1, τ_2, $-\tau_3$, $-\tau_4$ 60°) so providing some arithmetical justification for earlier views on conformational stability.[5] A second minimum is found at τ_1, τ_2, τ_3, τ_4 60° (Figure 5b), a conformation which is identical, in a different orientation, with that of τ_1, τ_2, τ_3, τ_4 180° (Figure 5c). The conformation corresponding to a third, slightly higher, minimum energy differs from that of Figure 5a in that one torsion angle is 120° rather than 60°. Local refinement at 2° intervals showed the lowest minimum to be characterised by τ_1, τ_2, $-\tau_3$, $-\tau_4$ 66°, the second by τ_{1-4} 60° (unchanged) and the third by (111, 60, −66, −66°). (Variation of the potential constants from the A_2 set affect the results slightly.) We refer to these three conformations as *M*1, *M*2, *M*3, their relative energies (little affected by small variations in torsion angle) being 0, 0·7, 1·1 kcal mol^{-1}. The reason for the relative stability of the two conformations of lowest energy can be seen by considering all six pair-wise interactions of the methoxy-groups. For *M*1 and *M*2 the conformations can be expressed as 2*GG*/4*GT*, 4*GG*/2*TT* respectively. *M*3 introduces interactions of higher energy characterised by (*e.g.*) τ_1 *ca.* 60 and τ_2 *ca.* 120°. Many more metastable conformations exist with energies not >3 kcal mol^{-1} above *M*3. The small energy differences are accentuated, *M*1 being stabilised, by the addition of polar interactions.

Both *M*1 and *M*2 conformations are found in simple structures, *M*1 in $Si(OMe)_4$,[17] $C(SMe)_4$,[18] and pentaerythritol tetranitrate,[19] *M*2 in pentaerythritol[20] itself and in its tetra-acetate.[21] In $N_6P_6(OMe)_{12}$, the local conformation at P(2) is *M*1, but is not quite ideal at either P(1) or P(3). At P(3) it is approximately *M*2, deviating from it in the way that *M*3 differs from *M*1: the two opposing sets of atoms, each ideally coplanar, are C(5),O(5),P(3),N(2),P(2) and C(6),O(6),P(3),N(3),P(1′). The conformation at P(1) lies between *M*1 and *M*3, one torsion angle [about N(3′)–P(1)] being *ca.* 40° less than the *M*1 ideal. This situation illustrates two limitations of the simple model. Deviations from ideal geometry, at least in $N_6P_6(OMe)_{12}$ and $N_8P_8(OMe)_{16}$, usually involve an approach to the *CT* conformation, the instability of which, relative to *GT*, is diminished as the angle at nitrogen is increased towards its real value. The second limitation is that most of the close non-bonded interactions (Table 5) involve the groups attached to P(1). The approximation of considering only local interactions may well be least good in this

---

[16] F. S. Mortimer, *Spectrochim. Acta*, 1957, **9**, 270; E. Steger and M. Kuntze, *ibid.*, 1967, **23A**, 2189; R. A. Nyquist, W. W. Muelder, and M. N. Wass, *ibid.*, 1970, **26A**, 769.

[17] M. Yokoi, *Bull. Chem. Soc. Japan*, 1957, **30**, 100.

[18] W. G. Perdok and P. Terpstra, *Rec. Trav. chim.*, 1943, **62**, 533.

[19] A. D. Booth and F. J. Llewellyn, *J. Chem. Soc.*, 1947, 837.

[20] R. Shiono, D. W. J. Cruickshank, and E. G. Cox, *Acta Cryst.*, 1958, **11**, 389.

[21] T. H. Goodwin and R. Hardy, *Proc. Roy. Soc.*, 1938, *A*, **164**, 369.

case. Nevertheless, consideration of the energy in terms of local conformations is evidently useful, as, out of a total of eleven crystallographically distinct environments in $[NP(OMe)_2]_n$ (n = 4, 6, 8), six are of the $M1$ type, one intermediate between $M1$ and $M3$, and two are $M2$ [one being at P(3) in $N_4P_4(OMe)_8$]. A different type, with one unfavourable (60, −60°, GG') conformation, is found at P(2) in $N_4P_4(OMe)_8$, and another, of somewhat higher energy, occurs at P(1) in $N_8P_8(OMe)_{16}$. These conformations are symbolised by $2GG/2GT/TT/GG'$, $GG/2GT/TT/2GG'$ respectively.

This discussion would be hardly more than descriptive if it only confirmed the stability of structures with staggered bonds, but more detailed consideration of the two conformations of lowest energy brings out a point of importance to all three structures, and with implications for other phosphazene structures also. The ideal $M1$ conformation has $\bar{4}$, and $M2$ has $\bar{4}2m$ symmetry, and the equality of torsion angles within each conformation which the symmetries imply allows an investigation of the effect of the variation of the angles at phosphorus on the energy. Preliminary calculations on a slightly more general $P(OMe)_4$, in which only a two-fold axis was assumed, showed that, for equal τ values, minimum energy was attained for $\alpha = \beta$ (Figure 6) for both $M1$ and $M2$, so that the higher symmetry is applicable in both cases, the further arithmetical treatment being thereby simplified. Conformational energies were calculated (A_2 constants) for a model with P–O 1·584, O–C 1·444 Å, P–O–C 120°, as a function of τ (0—180°) and α (45—66°). From a plot of V as a function of α, τ, the minimum energy of the $M1$ conformation was found at O–P–O(GG) 110·6°, O–P–O(GT) 108·9°, V 0 (arbitrary), τ 65°; for $M2$, O–P–O(GG) 112·3°, O–P–O(TT) 104·6°, V 0·49 kcal mol^{-1}, τ 58·4° (orientation as Figure 5b). On the basis of van der Waals interactions alone, there is therefore a tendency for the angle between P–O bonds in a GG conformation to expand at the expense of either the GT conformation ($M1$) or TT($M2$). We may expect that in such formally symmetrical compounds as $Si(OMe)_4$ there will be some distortion from regular tetrahedral angles at the central atom. The relevant structures are too inaccurately known to justify further comment.

In the methoxyphosphazenes, the endo- and exocyclic angles at phosphorus are not even ideally equal, and we need to consider how the 'normal' angles would be affected by non-bonded interactions. The primary stereochemistry of a molecule is determined by the σ-bonds, and the effect of π-interactions in a pair of bonds is, qualitatively, to increase the angle between them as a consequence of the increased electron density. If the σ-bonds are s–p hybrids, the angle between the opposite pair of bonds can then be expected to decrease, reflecting the redistribution of p orbitals. The quantitative relation between the expected angles is shown as a line in Figure 10. For the methoxyphosphazenes, the mean values of the endo- and exocyclic angles (118·3, 102·9°) are close to the curve (perhaps coincidentally), but individual pairs lie in separate groups, the low-angle group having GT conformations of the methoxy-groups, those of high-angle, with one exception, having GG conformations. These deviations are not wholly to be expected on the basis of the $P(OMe)_4$ model, which would give minimum energy for angles at phosphorus close to, but not exactly equalling, the tetrahedral value. Preliminary work with a $P(OMe)_4$ unit with unequal α and β showed a tendency for O–P–O(GG) to increase at the expense of OPO(GT). If we use the more realistic models $N_2P(OMe)_2$, or, especially, $(MeN)_2P(OMe)_2$, in which the non-bonded interactions of the remainder of the ring are simulated by those of two methyl groups, much larger effects are found in the same sense. We consider chiefly the $M1$ conformation (which is qualitatively recognisable even for unequal α, β), and for simplicity use a uniform torsion angle of 60°. Because of the reduced symmetry, it is necessary to examine two cases, the 'endocyclic' $[(MeN)_2P]$ and 'exocyclic' $[P(OMe)_2]$ groups being either both GG or both GT. Because oxygen and nitrogen have different potential constants, the minimum energy is no longer found for $\alpha = \beta$, but near those angles characteristic of the bond structure in the absence of the non-bonded interactions. The pairs of angles are not identical, however, and calculations show that the optimum O–P–O angle is greater in a GG than in a GT arrangement, when all the non-bonded interactions are included. The effect of the artificial methyl groups, essential to give meaning to two torsion angles, is not vital to the quantitative argument, which is perhaps why the simpler treatment leading to Figure 9 is useful.

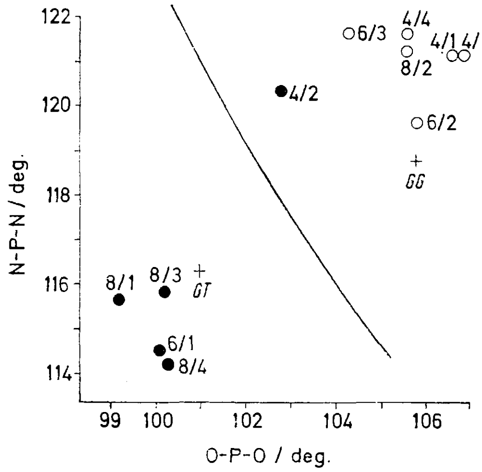

FIGURE 10 Relation between O–P–O and N–P–N angles. Solid line corresponds to s–p hybridisation [K. A. R. Mitchell, *J. Chem. Soc.* (*A*), 1968, 2683]. Points from structures; n/m means P(m) in $[NP(OMe)_2]_n$: open circles GG, solid circles GT conformations. Crosses are calculated points see (text)

For a particular set of numerical assumptions, based on A_2 constants and mean geometry, the calculated GG and GT angles are plotted in Figure 10. No attempt has been made to optimise agreement, because we have too little information to assess either the restraining effect of valence-deformation forces, or the polar contributions (which would stabilise a tetrahedral arrangement). Nevertheless, we believe we have demonstrated that the observed significant and systematic dependence of the O–P–O angle on local conformation embodied in Figure 10 is entirely explicable in terms of a combination of valence forces, which determine the order of magnitude of the angles, and non-bonded interactions which determine the deviations shown in Figure 10. The exceptional point [P(2) in $N_4P_4(OMe)_8$] is interesting. As Ansell and Bullen have pointed out,[4] there is no obvious reason why the conformation should be of an unusual type, but, with this particular arrangement of angular groups, the reason for the exceptional (and intermediate) value of the O–P–O angle can be seen in the fact that the exo- and endo-cyclic conformations are respectively *GT* and *GG*. The marked effects described earlier arise because such opposed groups are normally of the same type, and so reinforce each other.

We can now understand the mean geometry of the three molecules, embodied in Table 6. An N_4P_4 ring with the idealised 'saddle' conformation has $\bar{4}2m$ symmetry, so that each $(PN)_2P$ local conformation is of the *GG* type. Although there is only a small energy difference between *GG* and *GT* conformations, the latter seems better adapted for the formation of large rings and chains (since its terminal atoms are more spread out). The $N_6P_6(OMe)_{12}$ ring includes two well defined *GT* conformations [at P(1), P(1')]; in $N_8P_8(OMe)_{16}$ six out of eight are of this type, and it is the exclusive skeletal motif in the structure of the high polymer $NPCl_2$.[22] On the basis of this argument, if endocyclic and exocyclic *GG* and *GT* conformations are related as in the frequently occurring *M*1 conformation, the increasing proportion of *GT* arrangements in the ring should be accompanied by a decreasing mean angle at phosphorus both in the ring and between the exocyclic groups. This is what is found. The simultaneous increase of the ring angle at nitrogen is most likely an indirect effect; the change in hybridisation at phosphorus would shift σ-electron density towards nitrogen, which would tend to widen the angle.

Conclusion.—The foregoing semi-quantitative treatment of non-bonded interactions has provided explanations for: (1) the conformations of the exocyclic groups in relation to the local conformation of the ring, the occurrence of two main types, *GG* and *GT*, and the magnitudes of the torsion angles, and (2) the mutual variation of endocyclic and exocyclic angles at phosphorus, and the variation of their mean values with ring size. There may also be contributions from *d* orbitals, but clearly their importance is not crucial. They are required to explain the variation of ionisation potentials with ring size,[23] bond-length inequalities induced by a substituent,[24] and orientation behaviour.[25] Although it earlier appeared otherwise,[26] the two components of the double π-system in phosphonitrilic derivatives [27,28] do not differ greatly in strength, so that between them they provide little resistance to torsional motion about the ring bonds. The most likely effect of *d* orbitals, in the present context, is to facilitate angular variation at phosphorus, since a d_γ combination would allow orbital following not permitted by *s–p* hybridisation, but its quantiative extent is unknown. The use of *d* orbitals rarely determines primary stereochemistry, but has important effects on the quantitative details; the present investigation shows that non-bonded interactions can also be important, and have to be included in any detailed account of phosphazene geometry.

We thank the staffs of the Computing Laboratories at Huddersfield Polytechnic and Leeds University, and the Computing Centre (U.B.C.) for assistance, Professor M. R. Truter for crystallographic programmes, R. T. Oakley for help with the programming of the energy calculations, and the National Research Council of Canada for financial support (to N. L. P.).

[3/1992 *Received*, 28*th September*, 1973]

---

[22] E. Giglio, F. Pompa, and A. Ripamonti, *J. Polymer Sci.*, 1962, **39**, 293.

[23] G. R. Branton, C. E. Brion, D. C. Frost, K. A. R. Mitchell, and N. L. Paddock, *J. Chem. Soc.* (*A*), 1970, 151.

[24] W. C. Marsh and J. Trotter, *J. Chem. Soc.* (*A*), 1971, 573.

[25] N. L. Paddock, T. N. Ranganathan, and S. M. Todd, *Canad. J. Chem.*, 1971, **49**, 164.

[26] N. L. Paddock, *Quart. Rev.*, 1964, **18**, 168.

[27] D. W. J. Cruickshank, *J. Chem. Soc.*, 1961, 5486.

[28] D. P. Craig and N. L. Paddock, *J. Chem. Soc.*, 1962, 4118.